Chapter 7

CuO nanorods: a potential and efficient adsorbent in water purification

Pb(II)

Consumption for long time

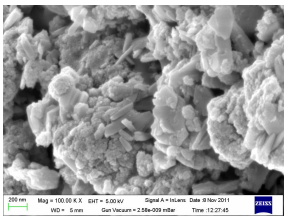

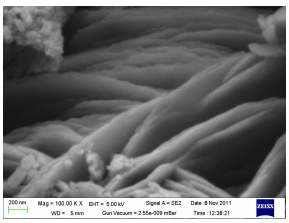

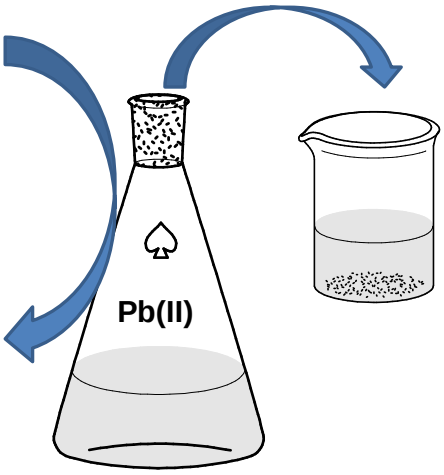

Lead free water

Chapter 7

7.1 Introduction

Water pollution is one of the major problems faced by the world today. Heavy metals in water is a alarming threat to human as well as other animals because of their toxicity, accumulation in the food chain and prevalence in nature. Heavy metals (Pb, Cr, Cd, Hg, As etc.) in diverse forms constitute some of the major inorganic pollutants and have many harmful effects on humans including other animals and environment. Lead is one of the major polluting heavy element which leads a lot to increase physiological, biochemical, and behavioral dysfunctions, particularly in children, which is contaminated through the activity like plumbing fixtures, ceramics, glass, cable coverings, manufacture of storage batteries, paints and pigments, oil, solder, lead smelting and mining.[1-4] Among the top 20 hazardous substances as suggested by the Agency for Toxic Substances and Disease Registry (ATSDR) and United States Environmental Protection Agencies (USEPA), lead is among one of the major pollutants.[5] Though, the prescribed permissible limit of lead regulated by WHO is 0.05 mgL^{-1}, in industrial water[6] it is found as high as 200–500 mgL^{-1}. Hence, remedial measures are required to reduce the lead levels to desirable concentration for drinking and other domestic purposes.

With the emergence of nanoscience and technology in the last decade, research has been initiated to exploit the unusual and unique properties of nanomaterials for environmental remediaion.[7-9] Among the various methods available for controlled synthesis, the "soft chemistry" routes, which are based on solution phase processes, are effective for the synthesis of nanostructured materials with well-controlled shapes, sizes, and structures.[10-14] There are some other techniques for synthesis of CuO NPs but requires more cost, time as well as involvement of more reagents.[15-17]

In this regard, we have adopted a simple, cost effective and eco-friendly method to synthesize copper(II) oxide NPs with rodlike symmetry. Thus synthesized NPs have subsequently been used for adsorption of lead from contaminated water. We have also described adsorption of copper oxide varying different parameters like initial concentration, adsorbent dosage, pH and competing ions. Adsorption isotherm also described and found to follow multilayered adsorption isotherm.

Parts of this chapter have been published in
Raul, P.K., Senapati, S., Sahoo, A.K., Umlong, I.M., Devi, R.R., Thakur, A.J., & Veer, V. *RSC Advances*, **4**, 40580--40587, 2014.

7.2 Experimental

7.2.1 Materials

A round bottom flask, other glasswares (borosil) along with reflux condenser and a heating mantle (REMI make, 200W) were used as experimental set up for synthesizing the copper (II) oxide NPs. Double distilled water was used throughout the experiments. All the chemicals including Cupric Chloride (Merck, India), Sodium Hydroxide (Merck, India), Hydrochloric acid (Merck, India), capping solvent, lead nitrate (Merck, India), Potassium dichromate (Merck, India), acetone (Sigma Aldrich Pvt. Ltd., Bangalore) and ethanol (Bengal chemicals Pvt. Ltd., Kolkata) were of analytical grade and used without further purification.

7.2.2 Synthesis

Copper(II) oxide NPs have been synthesized following our earlier reported procedure with some modification in order to get uniform smaller particles.[7] Cupric Chloride ($CuCl_2$), Sodium Hydroxide (NaOH) and capping solvent were mixed in 2:1:1 ratio with 200 mL ethanol in a round bottom flask fitted with a reflux condenser. The mixture was refluxed for 10 h (around 75 $^{\circ}$C) and allowed to cool to room temperature. Then the mixture was again refluxed for 5 h. The product was washed with double distilled water and acetone repeatedly. The dark brown precipitate was centrifuged and washed with ethanol, acetone and hot water respectively. Finally, the product was dried at room temperature and heated to 120 $^{\circ}$C in a vacuum oven in the absence of air and cooled to normal temperature. Final product was used for adsorption experiments.

7.2.3 Adsorption experiments

Standard lead stock solution of 1000 mgL^{-1} was prepared by dissolving 1.598 g of lead nitrate in 1L volumetric flask with double distilled water. 100 ml of each of working standard solution was taken in 250 ml conical flask and known weight of adsorbent material was added into it. The contents in the flask were shaken for 3 h on a mechanical shaker (IKA 400*ic* control) for different studies. The solution was centrifuged and the mother liquor was analyzed for residual contaminant concentration by Atomic Absorption Spectrometer. All adsorption experiments were conducted at room temperature (25 $^{\circ}$C± 0.1 $^{\circ}$C). Batch adsorption experiments were conducted to investigate the effect of various parameters like adsorbent dose, initial concentration, presence of interfering ions, pH etc. The specific amount of contaminant adsorbed was calculated from:

$Q_e = (C_0 - C_e) \times V / W$ ---------- (Equation 7.1)

Where Q_e is the adsorption capacity (mgg^{-1}) in the solid at equilibrium; C_0 and C_e the initial and equilibrium concentrations of metals/contaminant (mgL^{-1}) respectively; V the volume of the aqueous solution; W is the mass (g) of adsorbent used in the experiments.[18] The effect of solution pH on lead removal were studied by adjusting the pH of the solution either by using 0.1N HCl or 0.1N NaOH. In slightly acidic as well as basic pH, copper oxide NPs is stable and hence adsorption studies were carried out over the pH ranges of 5–11. The effects of the presence of competing ions such as calcium, sodium, hydroxide, chloride and iodide were studied at optimum experimental conditions (adsorbent dose $1gL^{-1}$, agitation speed 175 rpm, temperature 25 $^{\circ}C$ and contact time 3 h). The experiment for reusability of used copper oxide NPs was also performed. For this study, a certain amount of metal solution from working standard solution (200 and 500 μgL^{-1}) was initially allowed to adsorb on the NPs at wide range of pH. After adsorption the solid was separated by filtration and dried in air. The dried adsorbent was repeatedly subjected to the contaminant/metals removal/adsorption experiments in order to examine the extent of reusability.

7.2.4 Characterization

The details of the characterization techniques have been discussed in chapter 2.

7.3 Results and Discussion

Figure 7.1 shows the typical X-ray diffraction (XRD) profile in the 2θ range of 20^o to 70^o of the synthesized copper(II) oxide, show the presence of the different characteristics peaks and could be indexed on the basis of orthorhombic copper(II) oxide (JCPDS card no. 801268). It was matched from JCPDS file that the material was $Cu_2Cl(OH)_2$.

Transmission electron microscopy (TEM) (Figure 7.2a) shows that the nanorod is formed with diameter ~50 nm. Figure 7.2b clearly reveals lattice picture with approx. distance between two planes of 0.197 nm. Such a growth of nanorods in ethanol medium is not unusual and has already been observed in earlier reports.[19,20] Thus, for the present case, in all probability, ethanol acts as a soft template which facilitates the one dimensional growth of CuO nanorods.

The surface morphologies of copper(II) oxide nanorod before and after adsorption of lead from water were determined by FESEM images (Fig. 7.3a and Fig. 7.3b).

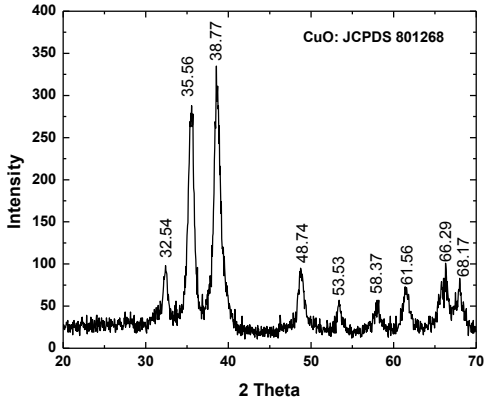

Figure 7.1: XRD pattern of Copper oxide NPs

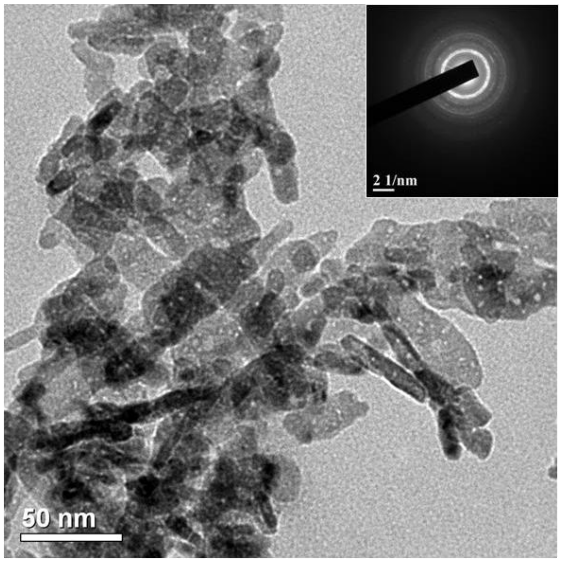

Figure 7.2(a): TEM and SAED images of copper(II) oxide NPs

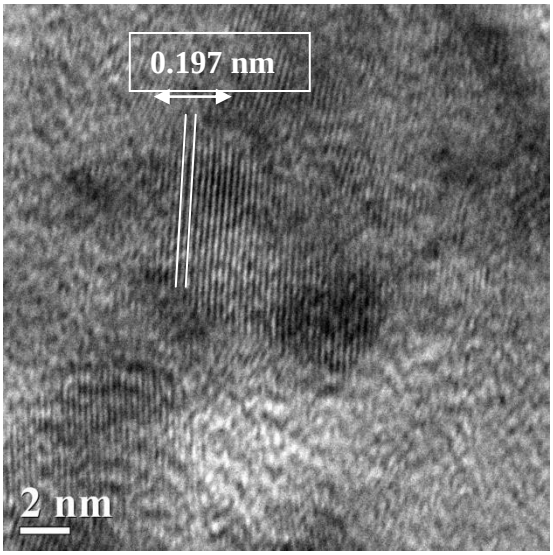

Figure 7.2(b): HRTEM image of copper(II) oxide NPs

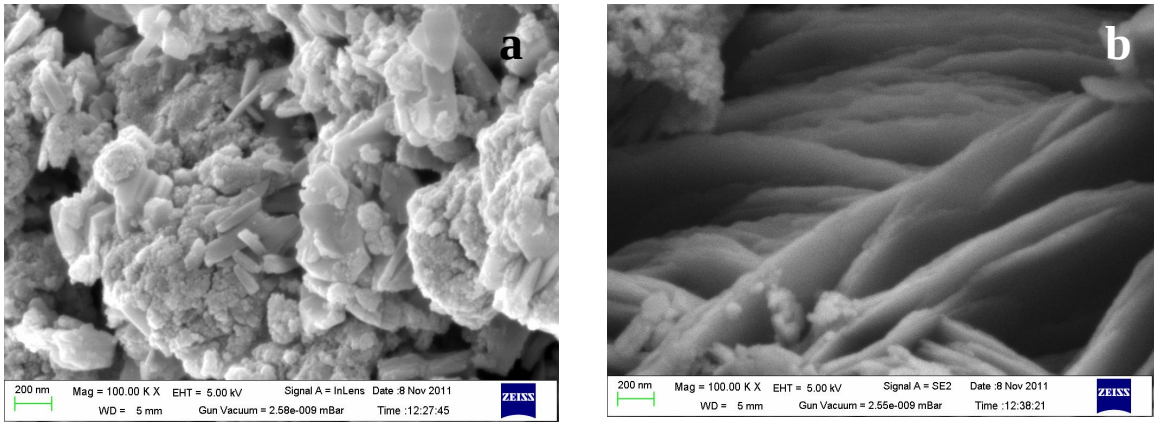

Figure 7.3: FESEM images of copper oxide NPs before (a) and after (b) adsorption of lead

Figure 7.4 revealed the presence of lead including other elements of CuO NPs, indicating that adsorbent was capable to remove lead from water. The specific surface area of the CuO NPs determined from BET surface area analyzer was 52.57 m^2g^{-1}. Fig. 7.5 showed the pore size distribution curve of adsorbent based on equilibrium adsorption isotherm at 77 K. It was observed from the figure that copper(II) oxide exhibited a wide distribution of pores. About 77.07% of total pores are in the range of pore diameter below 70 nm with total pore volume of 0.170 mL/g , which is an indication of high mesopore volume. The second fraction of pores were observed in the range, 70 to 150 nm with the pore volume of 0.026 mL/g (22.93% of the total pore volume) indicating the existence of the macropores.

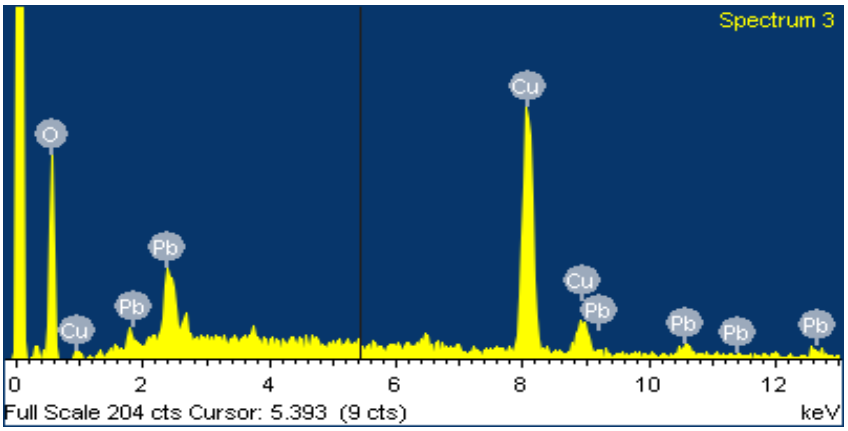

Figure 7.4: EDX pattern of copper oxide NPs after adsorption of lead

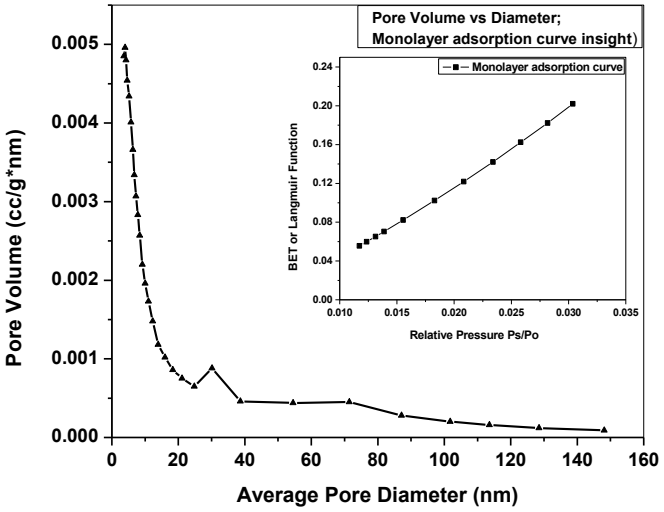

Figure 7.5: Pore volume distribution *vs* average pore diameter (Monolayer adsorption curve insight)

Figure 7.6 represents FT-IR spectrum of the freshly prepared cupric oxide samples materials. The bands at 2933 and 3432 cm^{-1} belong to the symmetric and asymmetric stretching vibration[21] of O-H bond respectively. The presence of bands at 523 cm^{-1} and 1011 cm^{-1} indicates different modes of bending vibration of Cu-O bond. Appearance of peak at 1639 cm^{-1} indicated stretching vibration of Cu-O bond of copper(II) oxide NPs.

7.3.1 Effect of sorbent dosage

The effect of adsorbent (CuO NPs) dosage on the adsorption of Pb(II) ion was studied using different dosage in the range, 0.1-4 gL^{-1}. The percentage removal of lead with different adsorbent dosage is shown in Figure 7.7. The percentage removal of lead is significantly increased with sorbent dosage, which is because of increase in the number of active sites as the dosage increases.[22] It was observed that adsorption remains constant after 1 gL^{-1} of adsorbent dosage. Hence, in all the subsequent experiments 1.0 gL^{-1} of adsorbent was fixed as the optimum dosage which could give reasonably good lead removal efficiency. Compared to other metal oxide, copper oxide NPs is found to have better efficacy towards removal of lead from water.[23,24]

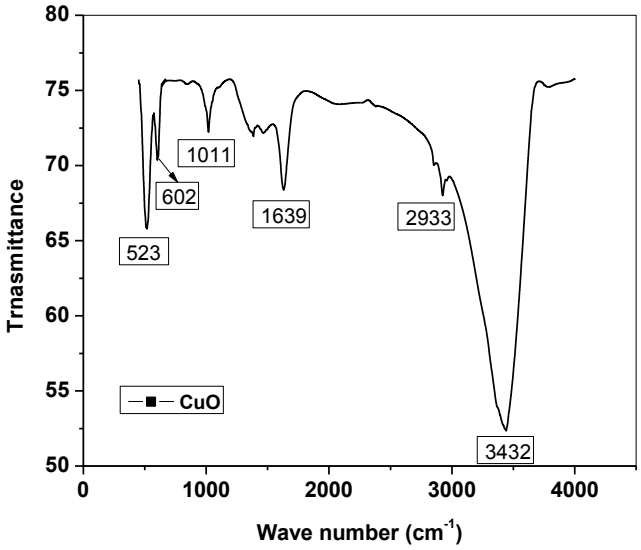

Figure 7.6: FT-IR spectrum of Copper Oxide NPs

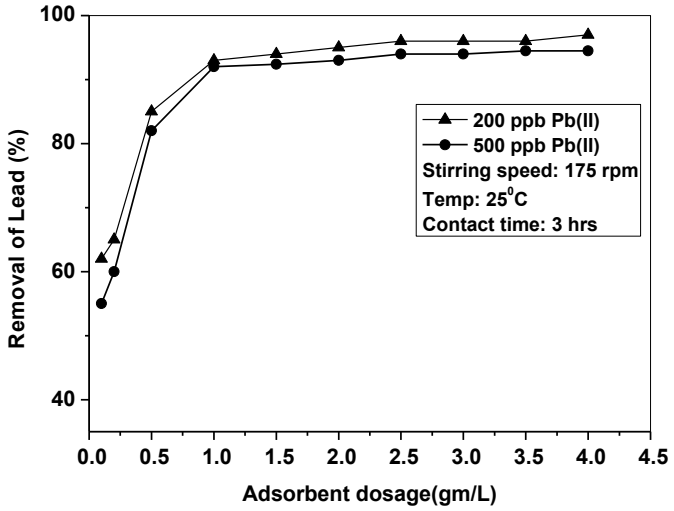

Figure 7.7: Variation of adsorbent dose on the removal of Lead

7.3.2 Effect of contact time

Figure 7.8 showed that the rapid adsorption of lead took place within 90 mins. Thereafter, the process slows down and almost reached equilibrium within 180 mins. No further appreciable adsorption takes (by less than 1%), place an increase in contact time up to 9 h, indicating that complete adsorption occurred within 3 h. Thus, further adsorption experiments were conducted taking duration of 3 h.[25,26]

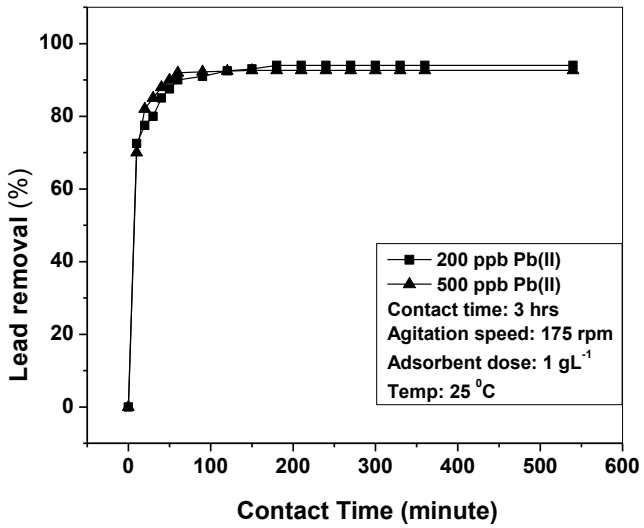

Figure 7.8: Removal of Lead *vs* contact time of agitation

7.3.3 Effect of initial concentration of adsorbate

To study the effect of initial concentration of lead ions on the extent of adsorption, dose of 1 gL^{-1} adsorbent dispersed in 2000 ppb of lead solution for contact time of 3 h and the findings are displayed in Figure 7.9. It has been observed that initially the rate of adsorption is fast and later it decreases with increase in concentration of lead. With increase in lead concentration, competition for the active adsorption sites increases and the adsorption process slows down.[27]

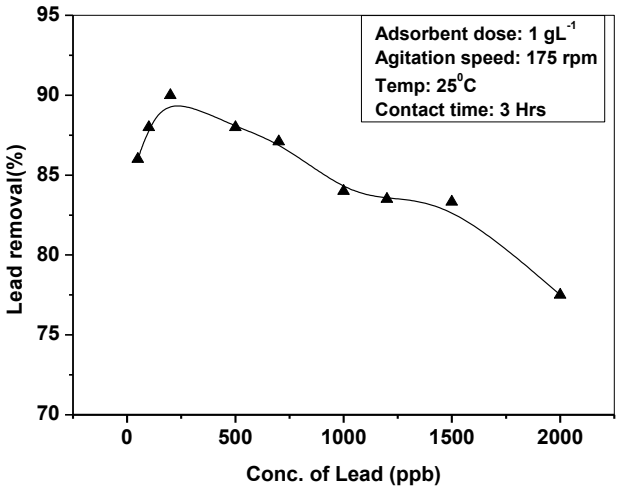

Figure 7.9: Variation of initial conc. of lead on the removal of Lead

7.3.4 Influence of pH and mechanism of sorption

Influence of pH on Pb(II) adsorption by CuO were investigated and the data are shown in Figure 7.10. From the Figure it is clear that Pb(II) adsorption by CuO nanorods is sensitive to pH variations.

However, for practical environmental application, the pH value of 8.3 has been taken as the experimental value as pH of drinking water should be within 6.5-8.5 (WHO/USEPA/BIS guidelines). In order to better assess the Pb(II) binding ability of adsorbents at various pH, the coefficient of distribution (K_d) value has been determined using the following mathematical expression.

$q = K_d C_e$ ---------- (Equation 7.2)

The K_d values thus obtained are plotted as a function of pH and the finds are shown in Fig. 7.11. It is important to mention here that higher the K_d value, better is the binding ability of the target pollutant.[28] In general, the K_d values in the range of 10^3 mlg^{-1} are considered good, and those above 10^4 mlg^{-1} are outstanding.[29] From the results (Fig.

7.11) it is clear that CuO nanorods are outstanding adsorbents in removing Pb(II) ions from aqueous solution.

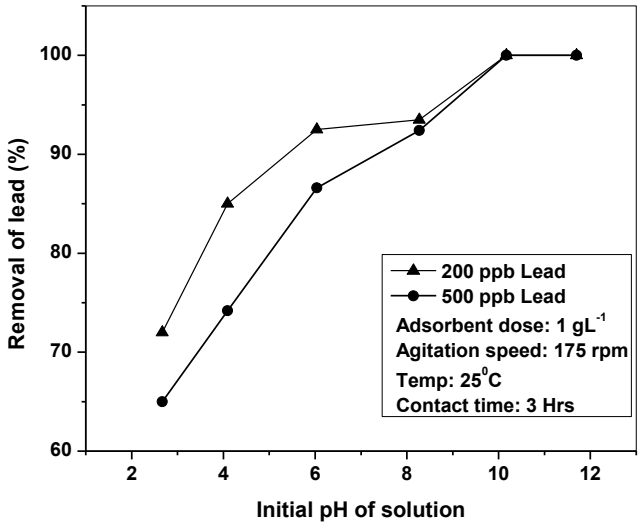

Figure 7.10: Removal of lead *vs* initial pH of the working solution

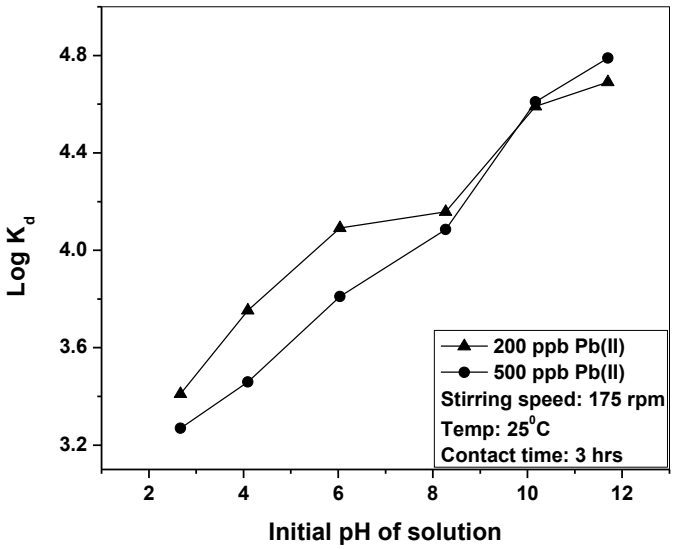

Figure 7.11: Plot of log K_d *vs* initial pH of lead solution

It is also observed that K_d *vs* pH plots of CuO NPs sharply increases with increase in pH indicating more sensitive nature of CuO to pH.

The extent of adsorption reportedly varies the solubility of the target metal. Therefore, it is important to know that whether Pb(II) removal at a particular pH has

happened through lead hydroxide formation or adsorption of divalent lead ion. Following equations are used to calculate the pH at which lead hydroxide starts to form.[30]

$Pb(OH)_2 \leftrightarrow Pb^{2+} + 2OH^-$ ---------- (Equation 7.3)

$$pH = 14 - \log \frac{\sqrt{Pb^{2+}}}{\sqrt{Ksp}}$$ ---------- (Equation 7.4)

$K_{sp} = [Pb^{2+}]\,[OH^-]_2$ ---------- (Equation 7.5)

Where K_{sp} is the solubility product of lead hydroxide which is 1×10^{-16} at 25 ^{0}C[31] and the $[Pb^{2+}]_{initial}$ =0.241µM (500 µgL^{-1}). Hence, the pH at which $Pb(OH)_2$ starts forming is calculated ~ 9.3 which rules out the precipitation of $Pb(OH)_2$ as the reason for Pb(II) removal in our case (pH<9.3).

The effect of pH on the efficiency of sorbent was studied at different pH from 2 to 11 by keeping other experimental parameters constant (adsorbent dose 1 gL^{-1}, contact time 3 h, rt) and shown in Figure 7.12. The percentage of lead removal was found more than 90% at basic pH (9.0) whereas it was less than 75% at acidic pH (4.1). The variation in uptake with respect to the initial solution pH can be explained on the basis of ZPC of the adsorbent.

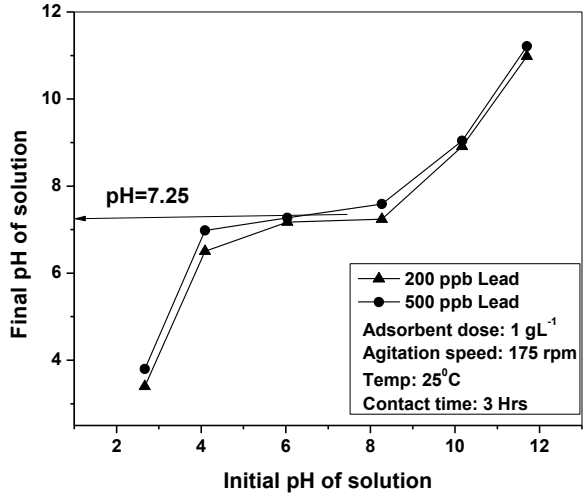

Figure 7.12: Plot of final pH *vs* initial pH of lead solution

To determine Zero Point Charge (ZPC) of CuO NPs, a plot made with initial pH of working lead solution *vs* final solution and shown in Figure 7.11 which shows that CuO NPs is neutral at pH 7.25 (=ZPC). Moreover, the maximum sorption capacity of the sorbent is found to be 3.31 mgg^{-1} at 25 ^{o}C. Adsorption of lead has been also studied taking activated carbon and it has been found that maximum adsorption capacity is 1.86

mgg^{-1}. Meikap *et al.*[32] also showed that activated carbon can be used as adsorbent for removal of lead with maximum adsorption capacity 2 mgg^{-1}.

When the adsorption system (lead solution/ copper oxide NPs) was operated at 7.25<pH<9.30, the reaction sites became negatively charged and contaminants with positive charge like lead are well adsorbed onto adsorbent. However, below pH=7, adsorption decreased as there is slight repulsion between positively charged cation as well as that from adsorbent surface. Thus, the mechanism of lead removal by adsorption of copper oxide NPs follows mainly physical rather than chemical as evident from enthalpy (ΔH^0) calculation.

7.3.5 Influence of competing anions

The contaminated drinking water may contain several common other anions, viz., OH^-, Ca^{2+}, Na^+ and I^- which could compete with lead ions during sorption process. Therefore, the adsorption was studied in the presence of diverse ions with varying initial concentrations of these ions keeping the $[Pb^{2+}]_{initial}$ as 200 and 500 ppb at rt.[33] Other experimental conditions e.g. agitation speed 175 rpm, temperature 25 $^{\circ}$C and contact time of 3 h are being kept constant and findings are displayed in Figure 7.13. It has been observed that with the increase in the concentration of these anions, removal of lead by the NPs decreases which may be due to a competition among them for the sites on the sorbent surfaces, which in turn is decided by the concentration, charge and size of the anions.[34] Figure 7.13 also indicates that the presence of competing anions like hydroxide ion (OH^-) has a significant effect on lead adsorption followed by calcium. The percentage of lead removal decreased sharply after 0.01 mM concentration of OH^- ion with both concentration of lead solution and adsorption goes below 60% in the presence of hydroxide ion at 1mM. Thus, at basic pH, the NPs possess higher affinity towards the hydroxide ion compared to lead. Adsorption of lead decreases profoundly in presence of the calcium ion although calcium ion is of almost same size and charge due to competing ion effect. However, the concentrations of competing anions in this study were far higher than those likely to be encountered in groundwater. Thus, from these observations it can be concluded that copper oxide NPs are able to remove lead from drinking water over a broad range of pH even at exceptionally high concentrations of the competing anions.

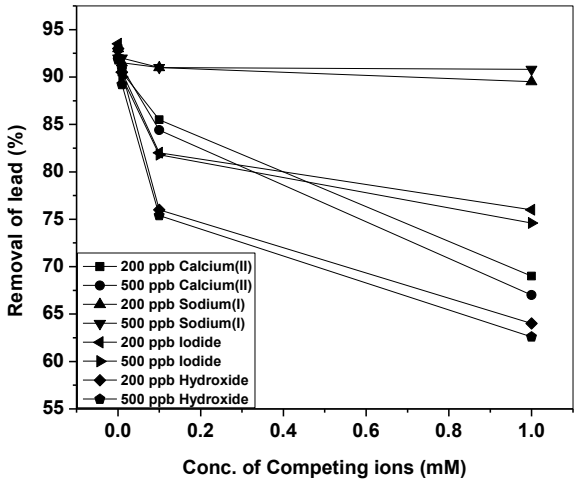

Figure 7.13: Effect of competing ions *vs* removal of lead

7.3.6 Temperature effect and thermodynamic study

It is observed that with increase in temperature the lead adsorption percentage was also found to be increased, indicating the endothermic behavior of adsorption. In addition, the temperature dependence of adsorption and its thermodynamic have been studied at three different temperatures *viz*. 298 K, 308 K, 318 K and the thermodynamic parameters viz. Gibb's free energy (ΔG^0), entropy (ΔS^0) and enthalpy (ΔH^0) changes for the adsorption process were determined by following equations.[35]

$$\Delta G° = \Delta H° - T\Delta S°$$ ---------- (Equation 7.6)

$$\log\left(\frac{q_e m}{Ce}\right) = \frac{\Delta S°}{2.303R} + \frac{-\Delta H°}{2.303RT}$$ ---------- (Equation 7.7a)

For unit adsorbent mass, Eq. (7a) became

$$\log\left(\frac{q_e}{Ce}\right) = \frac{\Delta S°}{2.303R} + \frac{-\Delta H°}{2.303RT}$$ --- ---------- (Equation 7.7b)

Where, q_e is the amount of lead adsorbed per unit mass of adsorbent ($\mu g g^{-1}$), C_e is the equilibrium concentration ($\mu g L^{-1}$), m is the adsorbent mass ($g L^{-1}$) and T is the temperature in Kelvin. q_e/C_e is called the adsorption affinity. The values of Gibb's free energy (ΔG^0) was calculated by knowing the enthalpy of adsorption (ΔH^0) (from plot of $\log(q_e/C_e)$ versus 1/T) and entropy of adsorption (ΔS^0). From these, ΔG^0 is determined applying Equation 6.6. Thus obtained thermodynamic parameters are summarized in Table 6.1 corresponding to solution $[Pb^{2+}]_{initial}$ =500 $\mu g L^{-1}$.

Table 7.1: Thermodynamic parameters for lead adsorption on CuO nanorods

Temperature (K)	ΔH^0 (kJmol^{-1})	ΔS^0 (kJmol^{-1}K^{-1})	ΔG^0 (kJmol^{-1})
298	-	-	-36.76
308	37.77	0.25	-39.23
318	-	-	-41.73

The +ve ΔH^0 and -ve ΔG^0 values clearly indicates the endothermic behavior of adsorption and spontaneous nature of the adsorption process respectively.[36] The low value of ΔS^0 indicates that no remarkable change in entropy occurred during the adsorption process.[37] However, +ve ΔS^0 value indicates the increased randomness at the solid-solution interface during adsorption. The value of ΔH^0 (37.77 kJmol^{-1}) indicates that the adsorption process is a physico-chemical adsorption process rather than a pure physical or chemical adsorption as heats of chemisorptions generally falls into a range of 80-200 kJmol^{-1}.

7.3.7 Adsorption isotherms

The adsorption isotherms are generally used to describe how adsorbate interacts with adsorbent at equilibrium and therefore it is critical in optimising the use of adsorbents. Two different isotherms have been adopted to understand the mechanism of adsorption for the removal of lead.

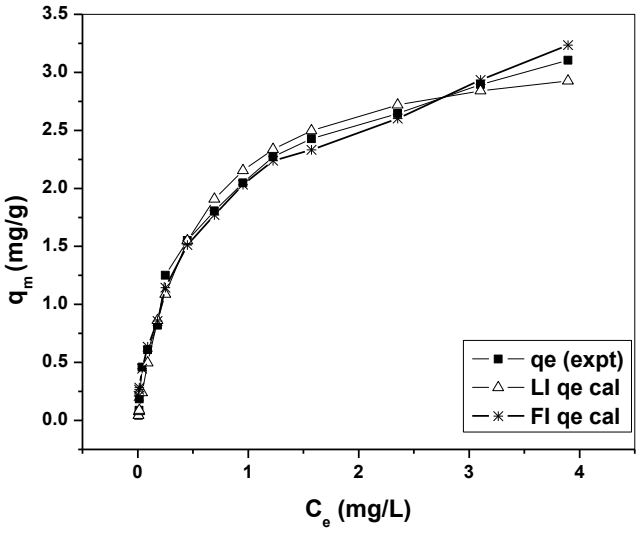

Figure 7.14: Equilibrium isotherm model for lead adsorption

Theoretical plots of each isotherm were tested for their correlation with the experimental results. Figure 7.14 showed the comparison of different isotherms studied at 25 °C.

The Langmuir equation assumes that no further adsorption can take place at that site if a Pb ion occupies a site. The Langmuir equation[38] is expressed as follows:

$$q_e = \frac{q_m b C_e}{1+bC_e}$$ ---------- (Equation 7.8)

Where, q_e is the equilibrium quantity adsorbed (mgg^{-1}), q_m is the maximum capacity of monomer adsorption (mgg^{-1}), Ce the equilibrium concentration of remaining Pb ions in solution (mgL^{-1}), b the adsorption equilibrium constant (Lmg^{-1}) related to the energy of adsorption. In order to predict the adsorption efficiency of the process, the dimensionless equilibrium parameter (R_L) was determined using the following equation:

$$R_L = \left(\frac{1}{1+bC_o}\right)$$ ---------- (Equation 7.9)

Where, C_0 is the initial concentration of working lead solution. The R_L value calculated was found to be lying between 0 and 1 which indicated favorable adsorption for all initial lead solution concentrations.

The Freundlich equation is an empirical equation and has the following form:[39]

$$q_e = K_f C_e^{1/n}$$ ---------- (Equation 7.10)

where, ($mg^{1-1/n}\, L^{1/n}\, g^{-1}$) is Freundlich constant indicative of the relative adsorption capacity of the CuO NPs and n is the empirical parameter representing adsorption intensity of the CuO NPs.

The maximum adsorption capacity was found to be 3.31 mg of Pb ions adsorbed per gram of CuO NPs with calculated adsorption equilibrium constant, b value of 1.96 Lmg^{-1}. The equilibrium adsorption data fitted better to Freundlich isotherm (R^2=0.9510) with root mean square error (RMSE) value being 0.0946 as compare to Langmuir isotherm (R^2=0.9431) with RMSE value being 0.1144). The value of K_f calculated was found to be 1.80 $mg^{1-1/n}\, L^{1/n}\, g^{-1}$

7.3.8 Lead desorption study

The exhausted copper oxide NPs were regenerated with eluents like dilute HCl and dilute NaOH.[40] All the regeneration experiments were carried out at room temperature.

Table 7.2: Regeneration study (adsorbent dosage: 1 gL^{-1})

Initial conc. of Pb(II) (mgL^{-1})	Conc. of adsorbed Pb (mgL^{-1})	Eluent Used	Conc. of eluent (M)	Conc. of Pb(II) in eluent after treatment (mgL^{-1})	Regeneracy of Lead (%)
200	196	NaOH	0.2	120	61.22
200	196	NaOH	0.5	140	71.43
200	196	HCl	0.2	160	81.63
200	196	HCl	0.5	194	Soluble
500	490	NaOH	0.2	320	65.30
500	490	NaOH	0.5	360	73.47
500	490	HCl	0.2	412	84.10
500	490	HCl	0.5	488	soluble

7.4 Conclusions

CuO NPs prepared through easy and soft chemistry route are found to be excellent candidates for removing Pb(II) from aqueous solutions. As far as practical applicability is concerned, CuO is more promising and is effective over a wide range of pH in presence of other competing/interfering ions. Reduced sensitivity to pH makes this adsorbent more attractive for cleaning up industrial effluents, especially effluents having low pH. The +ve ΔH^0 (37.77 $kJmol^{-1}$) and -ve ΔG^0 values clearly indicates the endothermic behavior of adsorption and spontaneous nature of the adsorption process respectively. The adsorption process is a physico-chemical adsorption process rather than a pure physical or chemical adsorption with +ve ΔS^0 value indicating the increased randomness at the solid-solution interface during adsorption. Equilibrium sorption data shows the sorption is multilayered on the heterogeneous surface of the nano adsorbent with maximum adsorption efficiency of the sorbent is 3.31 mgg^{-1} for lead at room temperature. Regeneration study reveals that the as-synthesized adsorbent can be regained and used multiple times by treating the spent adsorbent by an acid like HCl and alkali like NaOH.

References:

1. Banks, E.C., et al. *Neurotoxicology* **18** (1), 237--281, 1997.
2. Tunali, S., et al. *Sep. Purif. Technol*. **47 (**3**)**, 105--112, 2006.
3. Conrad, K. & Hansen, H.C.B. *Bioresour. Technol.* **98,** 89--97, 2007.
4. Eren, E., et al. *J. Hazard. Mater*. **161** (1-3), 677--685, 2009.
5. Moros, J.J., et al. *Anal. Chim. Acta*. **613** (2), 196–206, 2008.
6. Özcan, A.S., et al. *J. Hazard. Mater.* **161** (1), 499--509, 2009.
7. Goswami, A., et al. *Chem. Eng. Res. Design* **90** (6), 1387--1396, 2012.
8. Raul, P.K., et al. *J. Nanosc. Nanotech.* **12** (5), 3922--3930, 2012.
9. Thakur, S., et al. *J. Phys. Chem. C* **117**, 7636--7642, 2013.
10. Kharisov, B.I., et al. *RSC Adv.* **2** (25), 9325--9358, 2012.
11. Biswal, M., et al. *RSC Adv*. **3** (7), 2288--2295, 2013.
12. Zhang, J., et al. *Nanoscale* **5**, 9917--9923, 2013.
13. Cushing, B.L., et al. *Chem. Rev.* **104** (9), 3893--3946, 2004.
14. Chen, H., et al. *J. Phys. Chem.* **111** (49), 18033--18038, 2007.
15. Sun, S., et al. *Phys. Chem. Chem. Phys.* **15** (26), 10904--10913, 2013.
16. Asharf Shah, M., & Al-Farah, M.S. *Mater. Sci. App.* **2** (8), 977--980, 2011.
17. Wang, L., et al. *J. Mater. Chem.* **22**, 11297--11302, 2012.
18. Abdelwahab, O., et al. *Egypt. J. Aqua. Res*. **33** (1), 125--143, 2007.
19. Jia, R.P., & Zhang, Y.Q. *J. Nanoparticle Res.* **12** (8), 2717--2721, 2010.
20. Tsvetko, M.Y., et al. *Nanoscale Res. Lett.* **8** (1), 250--259, 2013.
21. Li, N., & Bai, R. *Ind. Eng. Chem. Res*. **44** (17), 6692--6700, 2005.
22. Mellah, S. & Chegrouche, S. *Water Res.* **31** (3), 621--629, 1997.
23. Hua, M., et al. *J. Hazard. Mater.* **211-212,** 317--331, 2012.
24. Sreeprasad, T.S., et al. *J. Hazard. Mater.* **186**, 921--931, 2011.
25. Ozer, A., & Ozer, D. *J. Hazard. Mater*. **100**, 219--229, 2003.
26. Sari, A., & Tuzen, M. *J. Hazard. Mater*. **171**(1-3), 973--979, 2009.
27. Naiya, T.K., et al. *J. Hazard. Mater*. **163**, 1254--1264, 2009.
28. Sharma, N., et al. *J. Hazard. Mater*. **163**, 1338--1344, 2009.
29. Yantasee, W., et al. *Environ. Sci. Technol.* **41** (14), 5114--5119, 2007.
30. AlDegsa, Y., et al. *Water Res.* **35** (15), 3724–3728, 2001.
31. Pauling, L., *A book on General Chemistry*, p. 456, Dover Publishing, 1970.
32. Dwivedi, C.P., et al. *J. Hazard. Mater*. **156** (1-3), 596--603, 2008.
33. Khin, M.M., et al. *Energy Environ. Sci.* **5** (8), 8075--8109, 2012.

34. Erdem, E., et al. *J. Coll. Interface Sci*. **280** (2), 309--314, 2004.
35. Namasivayam, C., & Kavitha, D. *Dyes and Pigments,* **54** (1), 47--58, 2002.
36. Xiong, C., et al. *Hydrometallurgy* **98** (3), 318--324, 2009.
37. Zeng, L., et al. *Water Qual. Res. J. Canada* **39** (3), 267--275, 2004.
38. Langmuir, I. *J. Am. Chem. Soc.* **40**, 1361--1403, 1918.
39. Freundlich, H.Z. *J. Phys. Chem*. **57A**, 385--470, 1906.
40. Viswanathan, N., et al. *J. Hazard. Mater*. **161**, 423--430, 2009.
41. Woman carrying water image in front page: https://encrypted-tbn3.gstatic.com/images?q= tbn:ANd9GcQUiUgbushfaf37MOTo2z7lyy0MC-GNmvAfJi5X-_aZCrXFup-G2 Q
42. Lead poisoning image in front page: http://d32ogoqmya1dw8.cloudfront.net/images/NAGTWorkshops/health/case_studies/lead_poisoning_symptoms_456.jpg
43. Glass water image in front page: https://encrypted-tbn3.gstatic.com/images?q=tbn:ANd9GcQlM6fvL3oKf741y-3QGN4Ofs84TugRm5O9zQg6EgYbHcr3jUiiBQ